

## **Modeling of Rocket Motor Ballistics for Functionally Graded Propellants**

Gregory Young  
Indian Head Division, Naval Surface Warfare Center  
Indian Head, MD

Hugh A. Bruck and Swaminathan Gowrisankaran  
Department of Mechanical Engineering, University of Maryland  
College Park, MD

### **Abstract**

Functionally Graded Solid Rocket Propellants are being developed at NSWC-Indian Head in conjunction with the University of Maryland. The approach being used treats these propellants as typical Functionally Graded Materials (FGMs), which by definition are structures that possess gradual variations in material behavior that enhance material and/or structural performance. For functionally graded propellants, Twin Screw Extrusion (TSE) processing is used to continuously vary the composition throughout a grain in a controlled manner. As a result, TSE processing allows the burning rates of propellants to be tailored as a function of burning web thickness. This in turn will allow for direct Thrust Magnitude Control (TMC) for a solid rocket motor, which has proven difficult to achieve in the past.

To realize the benefits of functionally graded propellants in rocket motors, an Inverse Design Procedure (IDP) is being developed that couples processing, property, and performance models with mathematical optimization techniques to enable designers to determine realistic gradient architectures that will meet the performance objectives. An essential part of this program is the development of a model that is capable of predicting the ballistic performance of functionally graded propellants. The development of such a model requires that new parameters be taken into account that would not be considered for a conventional solid propellant. For instance, not only will the burning rate change as a function of pressure and initial temperature, but the burning rate characteristics will also change as a function of position in the grain. Furthermore, the density and the thermochemistry associated with the graded architecture of the propellant will be changing in a continuous manner, whereas the grain will conventionally be represented by a web with discrete thickness. The details of the ballistics model and the effect on performance predictions related to discrete representations of continuously graded architectures will be discussed in the paper.

### **I. Introduction**

Solid propellants have provided one of the main propulsion sources for rockets of all types over the past 60 years. With all of the improvements that have been made in rocketry in the past century, solid rockets have reached a level of reliability to enable their routine usage<sup>1</sup>. In recent years the focus in the solid propellant industry has been to increase the performance of the propellants, improve their insensitive munitions (IM) characteristics, as well as to address some environmental concerns that come about from the toxicity of many rocket propellants' combustion products. While solid propellant rockets have proven to be relatively simple and reliable, one of their major drawbacks is the inability to throttle. Current solid propellants are limited to their own set of burning rate characteristics, which when combined with a certain grain geometry and nozzle configuration limits the possible thrust profiles achievable for a given rocket motor. Some work has been done with pintle nozzles to achieve some throttling capability, however this adds complexity and weight to what is ordinarily a relatively simple design<sup>2,3</sup>. Functionally Graded Solid Propellants (FGSPs) have the potential to change the entire landscape of solid rocket motor design.

By their very nature, FGSPs can provide an ability to create a whole new set of potential thrust profiles given very simple grain geometries. FGSPs can offer many advantages never before offered to the solid rocket motor community. Now very simple grain geometries can theoretically be used to obtain any thrust profile imaginable. For instance, an end-burning propellant grain configuration can be created to have a neutral, progressive, regressive, or any variance desired. A perforated grain can also be created to have any type of thrust profile as well. By using simpler grain geometries, the stress concentrations present in more complex rocket motor designs can be mitigated, reducing the likelihood of structural failures. Furthermore, FGSPs can offer the opportunity to improve propellant mass fraction by allowing configurations such as an end-burner to be used for a mission that it could not have been used before. A single propellant grain could theoretically act as both booster and sustainer in systems that require this type of performance. This is accomplished by intentionally varying the propellant composition in a controlled manner as a function of web thickness.

## **II. Objective**

The primary objective of this effort was to develop a ballistics model to predict the performance of rocket motors utilizing FGSPs. Initially, the model is designed as a simplistic ballistics model capable of predicting the pressure and thrust generated by a rocket motor from a given set of input parameters. The primary input parameters are propellant composition and burning rate as a function of web thickness. The model is designed to work in unison with property and processing models for the purpose of establishing an Inverse Design Procedure (IDP). The IDP couples processing, property, and performance models with mathematical optimization techniques to enable designers to determine realistic gradient architectures that will meet their performance objectives. One of the property models being incorporated into the inverse design procedure is the Petite Ensemble Model (PEM)<sup>4</sup>, which is used to attempt to predict burning rates of the propellants in an a priori fashion. These two models will be coupled with a Residence Distribution (RD) model that predicts the gradient architectures that can be processed using Twin Screw Extrusion (TSE) processing<sup>5</sup>. Once completed, the IDP allows the designer to start from the performance needs of a mission, and allow the IDP to calculate the required gradient architecture of the propellant grain to meet the performance needs of the mission as well as the processing conditions required for its fabrication. Therefore, it was critical to develop a ballistic model that can simply and accurately predict the performance of gradient architectures that will be encountered in the IDP.

## **III. Computational Model**

### **III.a Modeling of Burn Rate Properties**

For determining the material gradient and distribution in a propellant, a model is required to describe the combustion process. Based on the prediction of this model, the performance of the FGCEM can be optimized. For this investigation a steady-state combustion model called the Petite Ensemble Model (PEM) is used<sup>4</sup>. The PEM is based on a statistical treatment of the propellant surface with multiple flame structure centered about characteristic oxidizer particles. This model can be summarized by the following equations:

$$F_d = \frac{1}{(2\pi \ln \sigma)^{1/2}} \exp \left[ -\frac{1}{2} \left( \frac{\ln D_o - \ln \bar{D}_o}{\ln \sigma} \right)^2 \right] \quad (1)$$

$$\bar{r} = \int_{D_o} \frac{r_d F_d}{\alpha_d} d(\ln D_o) \quad (2)$$

$$R_p = \frac{1}{\bar{r}} \int_{D_o} \frac{R_{p,d} r_d F_d}{\alpha_d} d(\ln D_o) \quad (3)$$

$$R_v = \frac{1}{\bar{r}} \int_{D_o} \frac{R_{v,d} r_d F_d}{\alpha_d} d(\ln D_o) \quad (4)$$

where  $F_d$  is the overall oxidizer distribution function,  $D_o$  is the oxidizer particle diameter,  $\bar{D}_o$  is the mean oxidizer particle diameter,  $\sigma$  is the oxidizer distribution function mode width parameter,  $\bar{r}$  is the composite propellant mean burning rate,  $r_d$  is the burn rate for a pseudopropellant,  $\alpha_d$  is the pseudopropellant oxidizer mass fraction,  $R_p$  is the composite propellant pressure coupled response function,  $R_{p,d}$  is the pseudopropellant pressure coupled response function,  $R_v$  is the composite propellant velocity coupled response function, and  $R_{v,d}$  is the pseudopropellant velocity coupled response function. PEM predictions of the variation in burning rate with composition for TSE processed energetic materials can be seen in *Figure 1*.

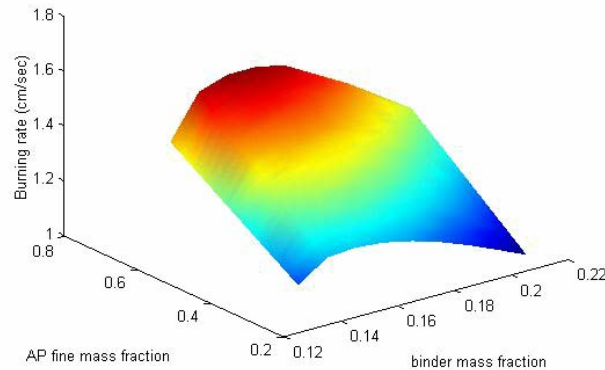


Figure 1. PEM prediction of variation in burning rate with composition for TSE processed energetic materials

### IIb. Modeling of Ballistic Performance

There are several challenges when one considers the ballistics of rocket motor using functionally graded propellants. First, the burning rate parameters are continuously changing. Preliminary results from the previous section indicate that burning rates may be intentionally altered by as much as 50%. Second, the thermochemistry of the propellant is also varying constantly as the composition changes. Finally the solid propellant density changes as the gradient architecture changes throughout the web of the propellant. Codes currently available to industry cannot take into account all of these challenges.

As a first attempt to predict the performance of solid rocket motors using functionally graded propellants, a computer code as been written that tries to take into account all of the problems that codes that predict performance of conventional solid propellants do not. Since this ballistics code is to be used as part of larger IDP, care must be taken to balance the accuracy of the results with the overall run-time of the code. Since the IDP may require many iterations, the run time of the ballistics code must be kept to a minimum while maintain reasonable accuracy.

Once the propellant gradients have been specified, the code predicts the performance of the rocket motor. The model assumes that each web gradient has unique burning rate properties, thermochemistry, and density. The code calculates the density of the propellant as a function of web thickness, runs the NASA CEA '00 computer code<sup>6</sup> to determine the thermochemistry at every single web gradient that was specified, and extracts all of the data that is of interest for ballistic calculations, such as the flame temperature,  $c^*$ , molecular weight of the gases, specific heat ratio, and gas constant. The code creates tables of these parameters versus burning web thickness.

Once the solid propellant density, and thermochemical calculations have been made the code is ready to handle the internal ballistics and performance calculations. During the ballistic calculations, the code references the tables created earlier as it monitors the propellant web burned. It marches in time, calculates web burned, and compares the web burned to the specified gradients. If the web burned is somewhere in between the gradients the code will linearly interpolate for the thermochemical properties of the propellant and burning rate parameters.

The ballistics routine predicting the performance of the rocket motors can be calculated from first principles. The control volume considered is depicted in Figure 2. The following assumptions were made when constructing the model.

1. Heat transfer was negligible.
2. The mass added by the burning propellant is at the adiabatic flame temperature of the propellant at the specified gradient.
3. The combustion gases behave as a perfect gas.
4. Frictional forces between the propellant surface and combustion gas was negligible.
5. Erosive burning was not considered.

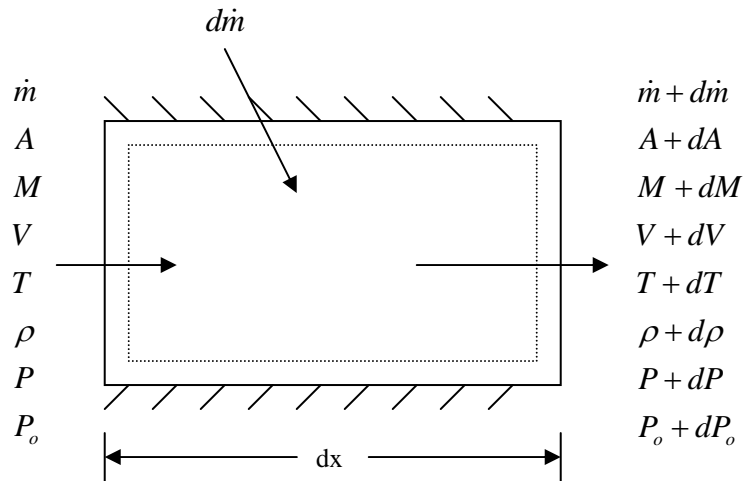


Fig. 2 Differential Control Volume

When considering these assumptions and logarithmically differentiating the principle equations<sup>7,8</sup>, the resulting equations are obtained.

State: 
$$\frac{dP}{P} = \frac{d\rho}{\rho} + \frac{dT}{T} \quad (5)$$

Continuity: 
$$\frac{dm}{m} = \frac{d\rho}{\rho} + \frac{dA}{A} + \frac{dV}{V} \quad (6)$$

Energy: 
$$C_p dT + \frac{d(V^2)}{2} + \frac{V^2}{2} \frac{d\dot{m}}{\dot{m}} = 0 \quad (7)$$

Momentum: 
$$\frac{dP}{P} + \frac{\gamma M^2}{2} \frac{d(V^2)}{V^2} + \gamma M^2 \frac{d\dot{m}}{\dot{m}} = 0 \quad (8)$$

Mach Number: 
$$\frac{d(M^2)}{M^2} = \frac{d(V^2)}{V^2} - \frac{dT}{T} \quad (9)$$

In addition, the static and stagnation pressure are related through isentropic flow relations, which when logarithmically differentiated yields:

$$\frac{dP_o}{P_o} = \frac{dP}{P} + \frac{\frac{\gamma M^2}{2}}{\left[1 + \frac{\gamma - 1}{2} M^2\right]} \frac{d(M^2)}{M^2} \quad (10)$$

The rocket motor geometry is broken into axial elements of equal size. Equations (5) – (12) are applied to each element for determining the incremental property contribution from each element. The incremental contribution is then combined with the incoming properties as is depicted in Figure 2. This combination then becomes the incoming set of properties for the next element. The incremental mass generation rate of combustion products,  $\dot{m}_g$  is related to the density of the products,  $\rho_p$ , the burn area,  $A_b$ , and the burning rate,  $r_b$ , as follows:

$$\dot{m}_g = \rho_p A_b r_b \quad (11)$$

The dependence of the burning rate on the chamber pressure,  $P_c$ , is specified in the traditional St. Robert's Burning Rate Law:

$$r_b = a P_c^n \quad (12)$$

where  $n$  is the burning rate exponent and the burn rate coefficient,  $a$ .

Once the calculation has been performed for each element, the final ballistic calculations can be made, starting with equation (13). The conservation of mass can be used to determine the change of mass,  $m$ , in the combustion chamber from the exiting mass flow rate,  $\dot{m}_e$ , and the total mass generation rate of combustion products,  $\dot{m}_{gt}$ , as follows:

$$\frac{dm}{dt} = \dot{m}_{gt} - \dot{m}_e \quad (13)$$

The exiting mass flow rate is determined from the exit throat area,  $A_t$ , using the choked flow assumption:

$$\dot{m}_e = \frac{P_c A_t}{c^*} \quad (14)$$

The equation of state for an ideal gas can then be used to relate the mass to the state variables, chamber pressure, chamber volume,  $V_c$ , and chamber temperature,  $T_c$ , as follows:

$$m = \frac{P_c V_c}{R_g T_c} \quad (15)$$

Differentiating (15) and combining it with (13) yields:

$$\begin{aligned} \frac{dm}{dt} &= \frac{d}{dt} \left( \frac{P_c V_c}{R_g T_c} \right) = \frac{P_c}{R_g T_c} \frac{dV_c}{dt} + \frac{V_c}{R_g T_c} \frac{dP_c}{dt} - \frac{P_c V_c}{R_g T_c^2} \frac{dT_c}{dt} - \frac{P_c V_c}{R_g^2 T_c} \frac{dR_g}{dt} \\ &= \dot{m}_{gt} - \dot{m}_e \end{aligned} \quad (16)$$

The instantaneous chamber volume,  $V_c(t)$ , is given by:

$$V_c(t) = V_{initial} + \int_0^t \frac{\dot{m}_{gt}}{\rho_p} dt \quad (17)$$

Differentiating (17) yields:

$$\frac{dV_c}{dt} = \frac{\dot{m}_{gt}}{\rho_p} \quad (18)$$

Substituting (18) into (16) and rearranging:

$$\frac{dP_c}{dt} = \frac{R_g T_c}{V_c} (\dot{m}_g - \dot{m}_e) - \frac{P_c}{V_c} \frac{\dot{m}_g}{\rho_p} + \frac{P_c}{T_c} \frac{dT_c}{dt} + \frac{P_c}{R_g} \frac{dR_g}{dt} \quad (19)$$

Where chamber pressure is solved incrementally by:

$$P_{c_{i+1}} = P_{c_i} + \frac{dP_c}{dt} \Delta t \quad (20)$$

The time step,  $\Delta t$ , is represented by:

$$\Delta t = \frac{1}{5} \tau \quad (21)$$

Where  $\tau$  is the propellant gas residence time in the combustion chamber and can be approximated by:

$$\tau = \frac{P_c V_c}{(1-n)(R_g T_c \dot{m}_e)} \quad (22)$$

Both the time derivatives of  $T_c$  and  $R_g$  are calculated via a one sided difference technique from the thermochemical data. For example:

$$\frac{dX_i}{dt} = \frac{X_i - X_{i-1}}{\Delta t} \quad (23)$$

Where  $X_i$  can represent state variables  $T_c$  or  $R_g$ .

The thrust of the rocket motor,  $F$ , is calculated in the following manner:

$$F = C_f P_c A_t \quad (24)$$

Where:

$$C_f = \sqrt{\frac{2\gamma^2}{\gamma-1} \left(\frac{2}{\gamma+1}\right)^{\frac{\gamma+1}{\gamma-1}} \left[1 - \left(\frac{P_e}{P_c}\right)^{\frac{\gamma-1}{\gamma}}\right]} + \frac{P_e - P_a}{P_c} \varepsilon \quad (25)$$

And:

$$\varepsilon = \frac{A_e}{A_t} = \frac{\left(\frac{P_c}{P_e}\right)^{\frac{1}{\gamma}} \left(\frac{2}{\gamma+1}\right)^{\frac{1}{\gamma-1}}}{\sqrt{\left[1 - \left(\frac{P_e}{P_c}\right)^{\frac{\gamma-1}{\gamma}}\right] \left(\frac{\gamma+1}{\gamma-1}\right)}} \quad (26)$$

Since  $\varepsilon$  is a known variable, (26) can be used to solve iteratively for the nozzle exit plane pressure,  $P_e$ . Once  $P_e$  is known, it is fed into (25) to solve for the thrust coefficient,  $C_f$ , from the isentropic expansion factor for the combustion products,  $\gamma$ .

#### IV. Discussion of Results

The ballistics code was written in the C programming language. When run on a desktop PC using 2 Pentium III 1.0 GHz processors, typical run times are on the order of 1 second for end-burning configurations, and 2 seconds for perforated configurations depending primarily on propellant grain web thickness. As the code was written, the industry standard SPP '97 computer code<sup>9</sup> was used to verify the results for conventional propellants. Figure 3 shows that very good agreement was achieved with the SPP results. Typically, the predicted pressures were within 1% once a "steady state" was achieved. Figure 3 displays the agreement for an end-burning propellant grain, but similar agreement has also been achieved with a center perforated propellant grain. The main discrepancies came during the chamber-filling phases. These discrepancies are being investigated. However, in this particular example, which is for a relatively small rocket motor, it appears that the chamber-filling event occurs too slowly in the SPP prediction. One possible reason for this is user error.

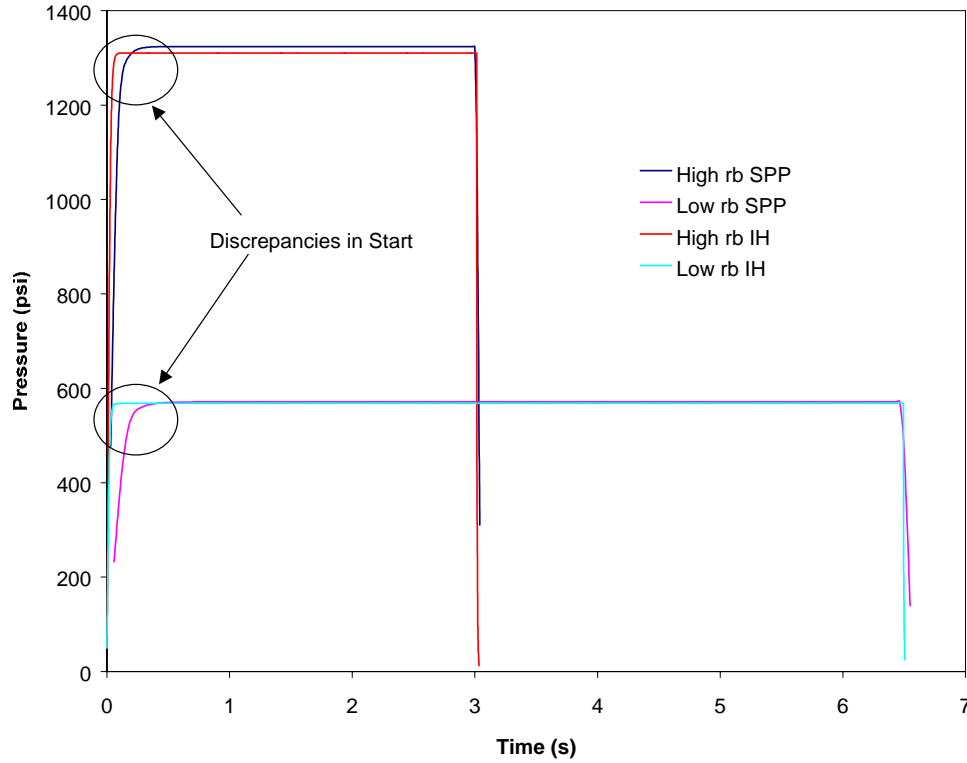


**Fig. 3 Verification of Results with SPP**

Figure 4 is an example of the output from the code when a graded propellant is used in an end-burning configuration. It shows the pressure and thrust history predictions for two separate end burning propellant grains, one with a conventional composite propellant, and another with a graded propellant. This example shows how using just one propellant configuration could create a boost-sustain system while utilizing a very simple grain geometry and potentially maximizing mass fraction.



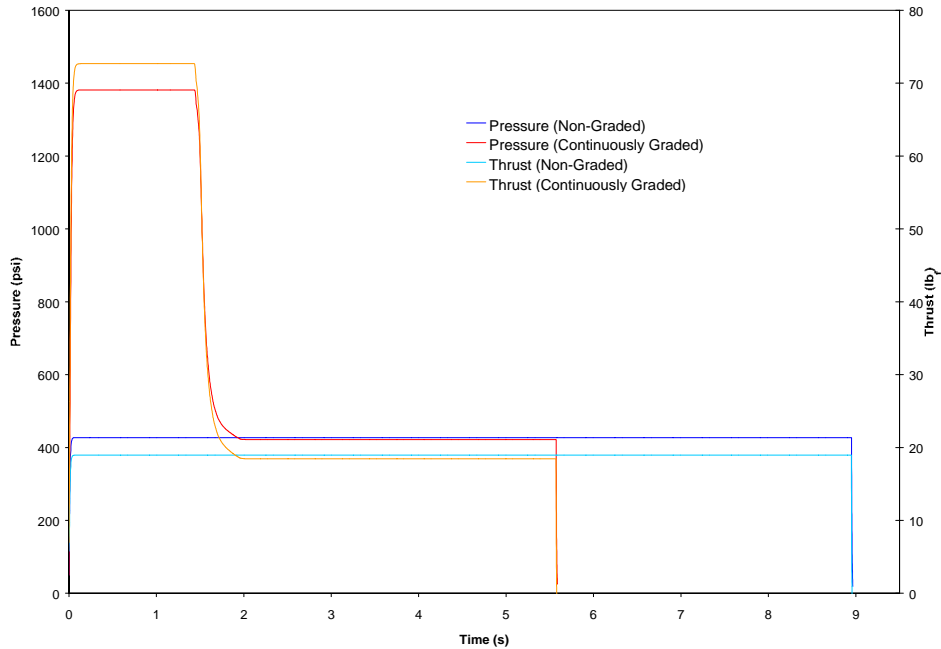


**Fig. 4 Performance Predictions for Graded and Conventional Propellants in an End-Burning Configuration**

Figure 5 shows the output from the ballistics code for both continuously graded propellants and conventional composite propellants when a center-perforated grain configuration is used. In both Figures 4 and 5, the propellant web starts out with a high burning rate and ends with a low burning rate. These high and low burning rates were considered the limits for this study, and as such calculations were performed for the high and low burning rate propellants if they were considered conventional propellants. The transition from high to low burning rates is done in a continuous manner. Curiously, in Figure 5 it is noted that the graded propellant experiences a “hiccup” in which the pressure actually becomes higher than the case of the high burning rate propellant. This phenomenon is a result of the gradient selected for this example and the changing burning surface area of the center-perforated grain. The results predicted by the ballistics code demonstrate that with sufficient computational resources, it may be possible to generate nearly any thrust profile desired by utilizing functionally graded solid propellants. This ballistics code, when coupled with the IDP discussed earlier will allow a designer, after making some basic sizing calculations, to select a mission thrust profile and input the profile into the IDP and have it return the processing conditions necessary to generate the corresponding gradient architecture.

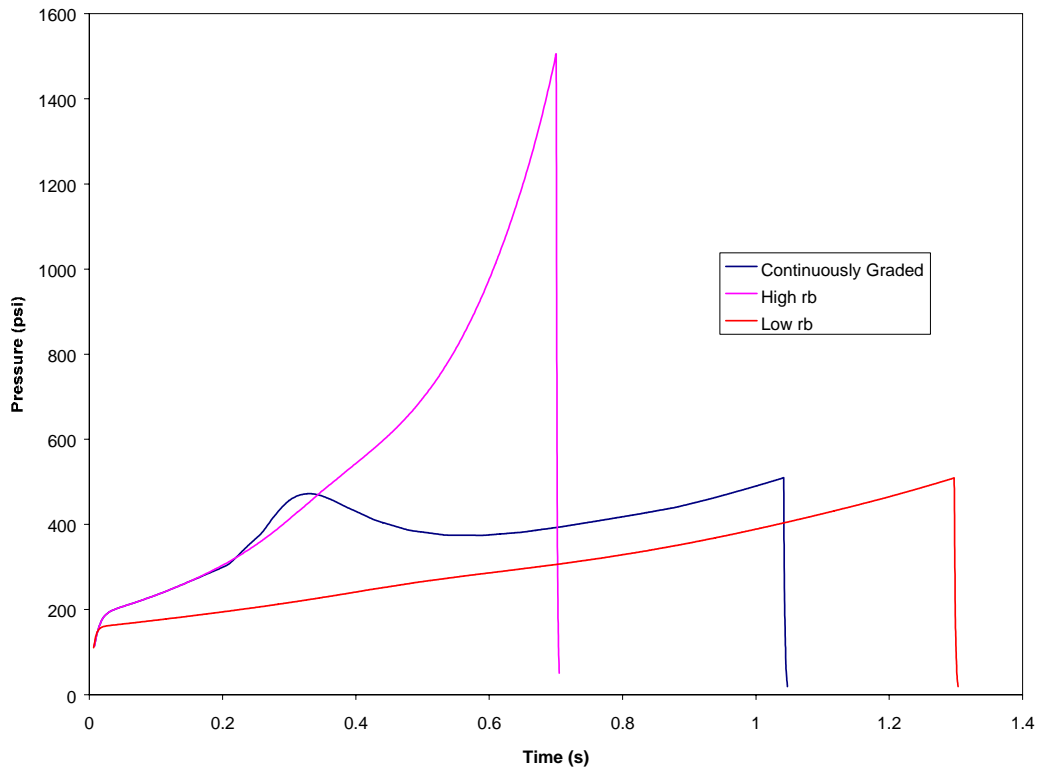


**Fig. 5 Performance Predictions for Graded and Conventional Propellants in a Center-Perforated Configuration**

## V. Conclusions

A ballistics code has been written to model the performance of rocket motors utilizing functionally graded solid rocket propellants. The code has been verified to give satisfactory accuracy for conventional solid propellants by comparing the results with the industry standard SPP '97 computer code while maintaining reasonable run times. This ballistics model when coupled with processing, property, and performance models with mathematical optimization techniques will form an Inverse Design Procedure (IDP) that will allow designers to define a performance requirement of a mission, make some simple scaling calculations, and allow the IDP to calculate the required gradient architecture of the propellant grain to meet the performance needs of the mission. At the time of publication, burn rate and small scale rocket motor testing was imminent. Appropriate modifications will be made if necessary to ensure that the ballistics routine will give results with a satisfactory level of accuracy to ensure success of the IDP.

## VI. Acknowledgements

This work was supported by Dr. James Short under ONR contract number N00014-00-1-0472, Indian Head-Naval Surface Warfare Center under contract no. TI01-9.

## References

1. D'Andrea, B., and Lillo, F., "Industrial Constraints as Evaluation Criteria in Developing Solid Space Propellants Using Alternative Energetic Materials," 33<sup>rd</sup> AIAA/ASME/SAE/ASEE Joint Propulsion Conference & Exhibit, July, 1997
2. Burroughs, Susan L., Michaels, R. Scott, Alford, Warren L., Spencer, Alan B., Peterson, Kevin L., "Demonstration of a Pintle Controlled Solid Rocket Motor in a Tactical Mission Application," 1996 JANNAF Propulsion Meeting, Albuquerque, New Mexico
3. Sims, J.D., Frederick, R.A., "Preliminary design of a hybrid propulsion multission missile system", *Journal of Spacecraft and Rockets*, 34, 186-191 (1997)
4. Glick, R.L. and Condon, J.A., "Statistical Analysis of Polydisperse, Heterogeneous Propellant Combustion: Steady State", *Thirteenth JANNAF Combustion Meeting*, CPIA Publication Number 281, 11, 313-345 (1976).
5. H.A. Bruck, F.M. Gallant, and S. Gowrisankaran, "Development of a Novel Continuous Processing Technology for Functionally Graded Composite Energetic Materials using an Inverse Design Procedure," *Proceedings of the 2002 SEM Annual Conference & Exposition*, 296-302 (2002)
6. McBride, B.J., and Gordon, S., "Computer Program for Calculation of Complex Chemical Equilibrium Compositions and Applications," NASA Reference Publication 1311, June 1996
7. Shapiro, A.H., "The Dynamics and Thermodynamics of Compressible Fluid Flow," Vol. 1, Ronald Press Company, New York, 1953
8. Armstrong, G.L., "An Analysis of the Instantaneous Performance Characteristics of Nozzleless Solid Rocket Motors," M.S. Thesis, Purdue University, May 1990
9. Dunn, S.S., Coats, D.E., "3-D Grain Design and Ballistic Analysis Using the SPP97 Code," AIAA Paper No. 97-3340, 33<sup>rd</sup> AIAA/ASME/SAE/ASEE Joint Propulsion Conference and Exhibit, Seattle, WA, July 6-9, 1997

### Nomenclature

a	Burning rate pre-exponential factor
$A_b$	Burning surface area
$A_e$	Nozzle Exit Area
$A_t$	Nozzle Throat Area
$C_f$	Thrust Coefficient
$C_p$	Constant pressure specific heat
$c^*$	Characteristic Exhaust Velocity
$\frac{dm}{dt}$	Rate of change of mass in the rocket motor
$\frac{dP_c}{dt}$	Rate of change of pressure in the rocket motor
$\frac{dR_g}{dt}$	Rate of change of gas constant in the rocket motor
$\frac{dT_c}{dt}$	Rate of change of temperature in the rocket motor
$\frac{dV_c}{dt}$	Rate of change of free chamber volume in the rocket motor
F	Thrust
$\dot{m}_e$	Mass exiting the rocket motor nozzle
$\dot{m}_g$	Incremental mass generated by burning propellant
$\dot{m}_{gt}$	Total mass generation rate by burning propellant
M	Combustion gas Mach number in the rocket motor bore
n	Burning rate exponential factor
$P_a$	Ambient pressure
$P_c$	Combustion chamber static pressure
$P_e$	Pressure at nozzle exit plane
$P_o$	Stagnation Pressure in Rocket Motor
$R_g$	Combustion gas constant
$T_c$	Combustion chamber temperature
V	Combustion gas velocity in the rocket motor bore
$V_c$	Combustion chamber free volume
$V_{initial}$	Initial combustion chamber free volume
$\epsilon$	Nozzle exit plane to throat area ratio
$\gamma$	Combustion gas specific heat ratio
$\rho$	Combustion gas density
$\rho_p$	Solid propellant density
$\Delta t$	Time step
$\tau$	Propellant gas chamber residence time